Available online at www.sciencedirect.com

ScienceDirect

Energy Procedia 4 (2011) 3997–4004

Energy Procedia

www.elsevier.com/locate/procedia

GHGT-10

Storage of CO_2 as hydrate beneath the ocean floor

Farhad Qanbari[a], Mehran Pooladi-Darvish[b,c,*], S. Hamed Tabatabaie[b], Shahab Gerami[d]

[a] *Tehran Faculty, Petroleum University of Technology, South Khosrow St., Sattarkhan Ave., 1453953153, Tehran, Iran.*
[b] *Department of Chemical and Petroleum Engineering, Schulich School of Engineering, University of Calgary, 2500 University Drive N.W., T2N1N4 Calgary, Alberta, Canada*
[c] *Fekete Associates Inc., Suite 2000, 540-5th Avenue S.W., T2P 0M2 Calgary, Alberta, Canada*
[d] *National Iranian Oil Company R&D, No.22, Negar Street, Vali-Asr Avenue, Vanak Square, 1969813771, Tehran, Iran*

Abstract

With the increasing concern about climate change, the public, industry and government are showing increased interest towards reduction of CO_2 emissions. Geological storage of CO_2 is perceived to be one of the most promising methods that could allow significant reduction in CO_2 emissions over the short and medium term. One major concern against geological storage of CO_2 is the possibility of its leakage. Carbon dioxide under the pressure and temperature conditions encountered in typical deep aquifers remains more buoyant than water. One process that could lead to permanent trapping of CO_2 is one that includes geochemical reactions leading to the formation of solid minerals. However, the time-scale of such reactions is perceived to be centuries to millennia. In contrast, the kinetics of CO_2-hydrate formation – that leads to trapping of CO_2 in the solid form – is quite fast, providing the opportunity for secure storage of CO_2. In this paper and its companion, two different geological settings that are suitable for formation of CO_2 hydrate are investigated. In this paper storage of CO_2 beneath the ocean floor is studied, while storage in depleted gas reservoirs is studied in the companion paper.

It has been suggested that CO_2 may be accumulated in the depressions *on* the ocean floor, where pressure and temperature conditions are such that either liquid CO_2 would accumulate or CO_2 hydrates would form. However, there have been significant concerns about the accompanying change in pH and its adverse effect on the ocean ecosystem. In this paper, permanent trapping of CO_2 at a depth of a few hundred meters *beneath* the ocean floor, where the CO_2 is thought to be of little or no harm to the ocean ecosystem, is studied.

Based on density calculations, Schrag and his co-workers [1,2] have shown that for oceans that are deeper than approximately 3000m, CO_2 density at the ocean floor is more than the surrounding water. With increased depth *below* the ocean floor and as a result of increased temperature, the density of CO_2 reduces faster than that of water such that at some depth below the ocean floor, CO_2 will be lighter than the surrounding water. Injection of CO_2 at such depths or deeper intervals will lead to rise of the CO_2 until it arrives at a depth where its density becomes heavier than water. The zone above this depth, where CO_2 becomes heavier than water is called the negative buoyancy zone. Beneath the negative buoyancy zone, the CO_2 is naturally trapped by a gravity barrier. Furthermore, as CO_2 is rising towards this depth, it could pass through conditions where CO_2 hydrates form. Formation of CO_2 hydrate will further reduce formation permeability and introduce a second barrier against CO_2 rise, even before it arrives at the boundary of the negative buoyancy zone.

Under dynamic conditions of injection and hydrate formation, the initial state of pressure and temperature is perturbed, affecting the negative buoyancy zone. Simulation studies are presented to investigate (i) the changes in pressure as a result of injection that could push CO_2 upwards into the negative buoyancy zone, and (ii) the increase in temperature as a result of formation of hydrates.

* Corresponding author. Tel.: +1 403 220 8779; fax: +1 403 284 4852.
E-mail address: pooladi@ucalgary.ca

doi:10.1016/j.egypro.2011.02.340

Through a case study, we report numerical simulation studies that indicate that injection of CO_2 at a depth of approximately 800m below the ocean floor leads to the rise of CO_2 until a depth of approximately 360m below the ocean floor, where hydrates will form reducing the formation permeability. Any CO_2 that might migrate further upwards could do so for another 135m before it arrives at the negative buoyancy zone. These simulation studies suggest that total CO_2 emissions of large power plants may be stored at such a site.

Keywords: CO_2 storage; Sequestration; Trapping; Negative buoyancy zone (NBZ); Hydrate formation zone (HFZ); Simulation; Ocean floor

1. Introduction

As an important source of CO_2 emissions [3], fossil fuels have retained their position as the leading components in the energy mix [4,5]. It is expected that they would provide the majority of world energy supplies in the coming decades [6]. Also, CO_2 is known as the main anthropogenic cause of global warming [7]. Many are of the opinion that the world cannot wait to find out definitiely if CO_2 emissions from fossil fuels may continue to grow without sever climate changes and that preventive and mitigating actions have to take place concurrently [8].

CO_2 capture and storage is one of the keys to assure the energy-hunger worlds of clean energy. Two major categories of the proposals for disposal of captured CO_2 are geologic and oceanic repositories [9]. Although the geologic sinks are the most readily accessible sites for CO_2 storage, they have some limitations with storage capacity and long-term maintenance of CO_2 sequestered in fluid form [10]. On the other hand, there are two concerns about direct injection of CO_2 into the ocean: leakage of CO_2 to the atmosphere, and unknown consequences of CO_2 for marine organisms [11].

In this study, storage of CO_2 in deep-ocean sediments is numerically modeled. Two important mechanisms that make this method superior to the other ones are: gravitational stability of liquid CO_2 and formation of solid hydrate, both of which reduce the risk of leakage.

2. Previous Studies

Koide et al. [12,13] proposed disposal of CO_2 in sub-seabed aquifers and identified three types of sub-seabed disposal of CO_2: shallow ($< 300m$), deep ($300 - 3700$m) and super deep ($> 3700m$). Schrag and his co-workers [1,2] proposed that at the high pressures and low temperatures common in deep-sea sediments (ocean depths greater than 3000m), CO_2 resides in its liquid phase. Furthermore, CO_2 hydrate formation will impede the flow of liquid CO_2. Therefore, deep-sea sediments provide a permanent reservoir for carbon dioxide captured from fossil fuel combustion. Goldberg et al. [14] proposed CO_2 sequestration in sediment-covered basalt aquifers under Juan de Fuca plate. Li et al. [15] modelled leakage rate of CO_2 in the sediments corresponding to ocean depths of $300 - 500$m, where CO_2 hydrate can be formed in the sediment. Rochelle et al. [16] proposed that cool underground storage of CO_2 appears to offer certain advantages in terms of physical, chemical and mineralogical processes.

3. Current Study

In this study, CO_2 storage in deep-sea sediments is developed and modelled by CMG STARS®2008. The phase behaviour of CO_2 hydrate and a kinetic model for the reaction is incorporated in the multi-phase multi-component thermal reservoir simulator. After some validation, two models are developed for deep and super-deep sub-seabed disposal and the results are analyzed.

4. Principles

4.1. Density of CO_2

Density of CO_2 is a strong function of temperature and pressure. NIST Standard Reference Data [17] has provided CO_2 properties over a vast range of pressures and temperatures. In this study, the liquid density function of CMG STARS is regressed for liquid CO_2 based on NIST over the required range of conditions. The equation for CO_2 density over the temperature and pressure ranges of $273 - 300$K and $30 - 45$MPa is obtained as

$$\rho_{CO_2}(p,T) = 1037.5\, e^{2.69\times10^{-6}(p-32)+2.873997353\times10^{-3}(T-280)-1.096031203(T^2-280^2)+5.4\times10^{-5}(p-32)(T-280)} \quad (1)$$

where $\rho_{CO_2}(p,T)$ is the density of liquid CO_2 (kg/m^3) at temperature, T (K) and pressure, p (MPa). This equation gives density of liquid CO_2 with maximum error of 0.2% for the above range.

Figure 1a illustrates the phase behaviour of CO_2 (Red line) [18], the isochors for its pure liquid phase (Dotted lines) [17], and a sample temperature distributions in the ocean in low to middle latitudes [19] and its sediments (geothermal gradient of 0.03 K/m). This figure shows that at a certain depth (of approximately 2600m in Figure 1a), the density of CO_2 exceeds the density of water. Below the seabed, the density of CO_2 decreases as temperature increases, such that at a particular depth (of approximately 700m below the seabed in Figure 1a), the density of CO_2 becomes less than that of ocean water, once again. Therefore, in this situation the density of CO_2 remains more than that of ocean water between the seabed and this second depth (of 700m below the seabed in Figure 1a). The region of the sediment from the seabed to the neutral buoyancy level in the sediment is called Negative Buoyancy Zone (NBZ) [1]. This zone in the sediment provides a natural trap for any CO_2 that may be injected further below.

4.2 CO_2 Hydrate

Aqueous clathrates or clathrate hydrates (known as gas hydrates) are those cage-like inclusion compounds having water as the host species [20]. CO_2 forms structure I (sI) hydrate [21] with ideal hydration number of 5.75. Figure 1b shows the phase behaviour of CO_2 hydrate (using CSMGem 1.10) (the Red curve). Q_1 and Q_2 in Figure 1b are the quadruple points where hydrate formation or dissociation occurs with another phase change concurrently. The points H_1 and H_2 are the intersection of temperature profile with hydrate phase equilibrium curve in ocean and sediment, respectively. Similarly, the points N_1 and N_2 are the points of intersection of temperature profile with iso-density line for CO_2 and water in ocean and sediment, respectively. X_1 is the intersection of iso-density line for CO_2 and water with hydrate phase behaviour.

In the sediment, temperature increases based on geothermal gradient and increases the pressure requirement for stability of hydrate. At a special point in the sediment the equilibrium pressure exceeds the pressure provided by the water head. If hydrate is stable on the seabed, hydrate formation zone (HFZ) is defined as the zone of stability of hydrate in the ocean sediment [1]. Because of the plugging of the pore space with solid hydrates, this zone acts as a cap for the CO_2 stored underneath.

CMG STARS can handle the reactions between the components in any phase present in the system. Furthermore, solid phases can be defined in the pore space. Therefore, hydrate formation and decomposition reactions, in which water, guest components and solid hydrate are involved, can be defined in this software. Using the pressure ratio instead of K-value, the kinetics of hydrate formation and decomposition reactions based on the general kinetics formula of this software [22] is presented as follows

$$r = r_r e^{-E_{act}/R.T} \varphi_f^2 \rho_{CO_2} \rho_w S_{CO_2} S_w p_{eq} \times \mathrm{Max}\{0, \pm(p/p_{eq} - 1)\} \quad (2)$$

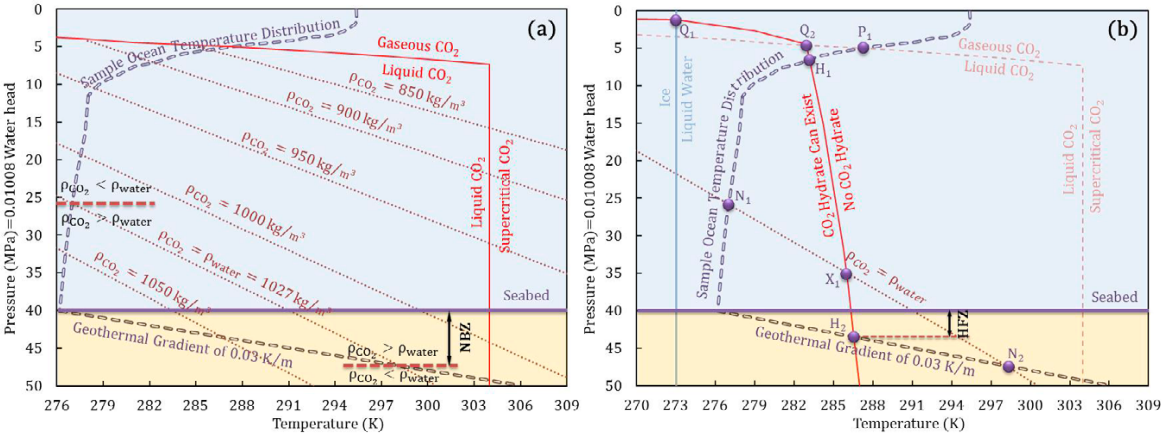

Figure 1 Schematic illustration of: a. Negative buoyancy zone (NBZ), b. Hydrate formation zone (HFZ)

where r is the rate of hydrate formation and decomposition ($gmole/m^3.day$), r_r is the constant of reaction ($(gmole/m^3)^{-1}/day.kPa$), φ_f is the effective porosity (fraction), ρ_{CO_2} and ρ_w are the densities of CO_2 and water ($gmole/m^3$), respectively, S_{CO_2} and S_w are the saturations of CO_2 and water (fraction), p is the pressure of the system (kPa), and p_{eq} is the equilibrium pressure (kPa) corresponding to the temperature of the system. The sign '+' is for hydrate formation and '−' for hydrate decomposition. The term 'Max' seeks for the conditions at which the reaction is active.

4.3 Variable Permeability

The permeability of the porous media can change due to formation and/or decomposition of hydrates. This change can be accounted for through use of the Carmen-Kozeny relation (Equation 3) available in CMG STARS [22].

$$k/k_0 = (\varphi/\varphi_0)^{\varepsilon}[(1-\varphi_0)/(1-\varphi)]^2 = (1-S_H)^{\varepsilon}[(1-\varphi_0)/(1-(1-S_H)\varphi_0)]^2 \quad (3)$$

where φ and φ_0 are the current and initial porosities respectively, and ε is the fitting parameter with the value ranging from 1 to 10. In the absence of permeability hysteresis in hydrate reformation/dissociation, this model behaves similar to that of the Masuda, which relates permeability to hydrate saturation [23,24].

4.4 Other Mechanisms

Other mechanisms that help permanent storage of CO_2 in deep-ocean sediments are: blanketing sediments just beneath the seabed [14,25,26], solution of CO_2 in water [27,28,29], gravitational stability of carbonated water [28,30,31], and geochemical trapping of CO_2 [32,33]. These mechanisms are not considered in this stage of the studies.

Cooler temperature at the upper parts of the ocean sediment would also increase the viscosity of liquid CO_2 [16] which reduces its flow rate in the formation. Viscosity of liquid CO_2 at average pressure of $28MPa$ and temperature range of $273-300K$ is obtained from NIST and tuned based on the STARS viscosity formulation as

$$\mu_{CO_2} = 0.005043e^{912.8/T} \quad (4)$$

where μ_{CO_2} is the density of CO_2 in cp, and T is the absolute temperature in K. The error in viscosity calculation by Equation 4 is less than $0.6\ \%$.

5. Storage Options

This section introduces a classification strategy for ocean depth for CO_2 disposal based on relative thicknesses of NBZ and HFZ. Figure 2 shows the variation of the thicknesses of NBZ and HFZ with ocean depth for temperature of $275K$ at the seabed and geothermal gradient of $0.03\ K/m$ in the ocean sediment. The points N and H are defined as the first ocean depths at which NBZ and HFZ appear, respectively. With increased ocean depth beyond these two points the thicknesses of the relevant zones increase. In the case shown in Figure 2, the ocean depth required for formation of hydrate is less than $1000m$, while that for having a NBZ is $2330m$. However, due to low pressure-dependency of hydrate phase behaviour in presence of liquid CO_2, the thickness of HFZ grows much slower than NBZ. Therefore, there would appear a particular ocean depth, beyond which the thickness of NBZ becomes larger than that of HFZ. This depth is characterized with an X on Figure 2.

Table 1 lists the location of these points for temperatures of 275, 280 and $285K$ at the seabed and the values of geothermal gradient of 0.02, 0.03 and $0.04\ K/m$ at static conditions. Ocean depth required for N, H and X increases whereas the thickness of NBZ and HFZ decreases with increasing the value of ocean floor temperature.

In this study four zones are defined for storage of CO_2 in the ocean sediments, in terms of ocean depth, based on Figure 2 and Table 1: (i) shallow (ocean depths lower than N and H), (ii) intermediate (ocean depth between H and N), (iii) deep (ocean depth between N and X), and (iv) super-deep (ocean depth greater than X). The names for the categories are adopted from Koide et al. [12], adding the second category. However, the approach to the classification and consequently, the depth ranges are different.

In shallow sub-seabed disposal of CO_2, the conditions of the seabed and its sediments are not suitable for formation of CO_2 hydrate and CO_2 may be in gaseous state and/or liquid state more buoyant than water. The sediments at intermediate zone of the ocean provide just HFZ. In deep sub-sea disposal of CO_2, the sediment possesses both NBZ and HFZ. Furthermore, the thickness of HFZ is more than that of NBZ in contrary to super-deep case.

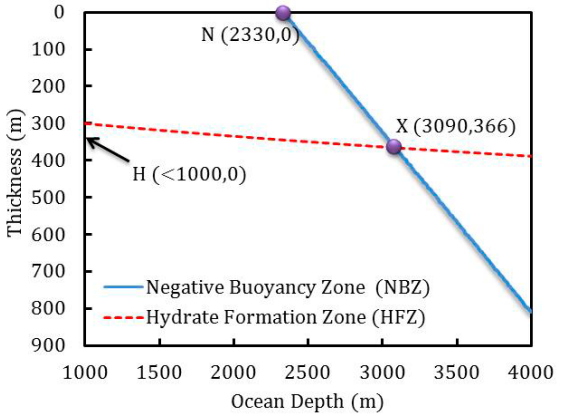

Figure 2 Comparison of the change of the thicknesses of NBZ and HFZ

Table 1 H, N, and X for different ocean and sediment temperature distributions

			Temperature gradient (K/m)		
			0.02	0.03	0.04
Temperature at the seabed (K)	275	N	2330	2330	2330
		H	<1000	<1000	<1000
		X	(2910, 549)	(3090, 366)	(3180, 275.5)
	280	N	2845	2845	2845
		H	< 1000	< 1000	< 1000
		X	(3160, 290)	(3255, 199)	(3305,149.5)
	285	N	3355	3355	3355
		H	2295	2295	2295
		X	(3410, 49)	(3425, 32.5)	(3430, 24.5)

This study uses the advantages of both hydrate formation and gravitational stability of liquid CO_2 to store CO_2 permanently in the ocean sediments. Therefore, deep and super-deep sub-seabed disposal of CO_2 are favorable. A numerical model is developed to predict the fate of CO_2 in ocean sediments at these conditions.

6. Model Development

Using CMG STARS, a three-component and three-phase model is developed to simulate fluid flow, heat transfer, and formation and decomposition reactions. In the model of this study, components include water in the aqueous phase, CO_2 in the liquid-CO_2 phase and CO_2 hydrate in the solid phase. CO_2 hydrate forms as a result of reaction between water in the aqueous phase and the CO_2 in the CO_2-liquid phase. Solubility of CO_2 in water is ignored.

The properties of the pure components are obtained using NIST Standard Reference Data [17]. Hydration number and density of hydrate is assumed 7.3 (corresponds to the non-ideal stoichiometric reaction) [27,34] and $1100\,\mathrm{kg/m^3}$ [27], respectively. The frequency factor, enthalpy, and activation energy of hydrate formation reaction are $10^{20}((\mathrm{gmole/m^3})^{-1}/\mathrm{day.kPa})$, $48.4\,\mathrm{KJ/gmole}$, and $81084.2\,\mathrm{KJ/gmole}$, respectively.

Simplified models were built to validate the model for correct representation of the two key mechanisms of CO_2 hydrate formation (in HFZ) and gravitational stability of liquid CO_2 (in NBZ). In the following, we present two models that were developed to simulate the flow of CO_2 in the sediment for deep and super-deep cases.

A cylindrical geometry with thickness of 1300m and radius of 80km (to represent an extended seabed) is considered to represent the storage reservoir. The porosity, horizontal and vertical permeability values are taken to be 0.15 (fraction), 100mD and 20mD, respectively. Furthermore, the Carmen-Kozeny constant, rock compressibility, rock heat capacity and thermal conductivity are assumed to be 5 (dimensionless), $5\times10^{-7}\mathrm{kPa^{-1}}$, $2.45\times10^{6}\,\mathrm{J/m^3.K}$ [35,36], and $2.0736\times10^{5}\,\mathrm{J/day.m.K}$ $(=2.4\,\mathrm{W/m.K})$ [37]. The upper boundary of the reservoir is designed to be at constant pressure representing the ocean. The boundary conditions on the periphery and the bottom of the reservoir are considered to be a no flow boundary.

In Case 1 (deep ocean), the ocean depth for injection is assumed to be between N and X (2800m, in this study), where the thickness of HFZ (360m) is more than the thickness of NBZ (225m). For Case 2 (super-deep ocean) the ocean is deeper than X (3500m, in this study) where the thickness of NBZ (565m) is more than the thickness of HFZ (376m). Liquid CO_2 (at a temperature of 288K) is injected at sediment depths of between 750 and 800m below the seabed. The maximum injection rate is 3000 ton/day and the maximum pressure at the wellbore is allowed to be approximately 5 percent greater than the initial pressure.

7. Results

In both cases considered here, the CO_2 is injected below both NBZ and HFZ. The horizontal and vertical flow of CO_2 in the formation is affected by the horizontal pressure gradient and the buoyancy gradient. Formation of hydrate

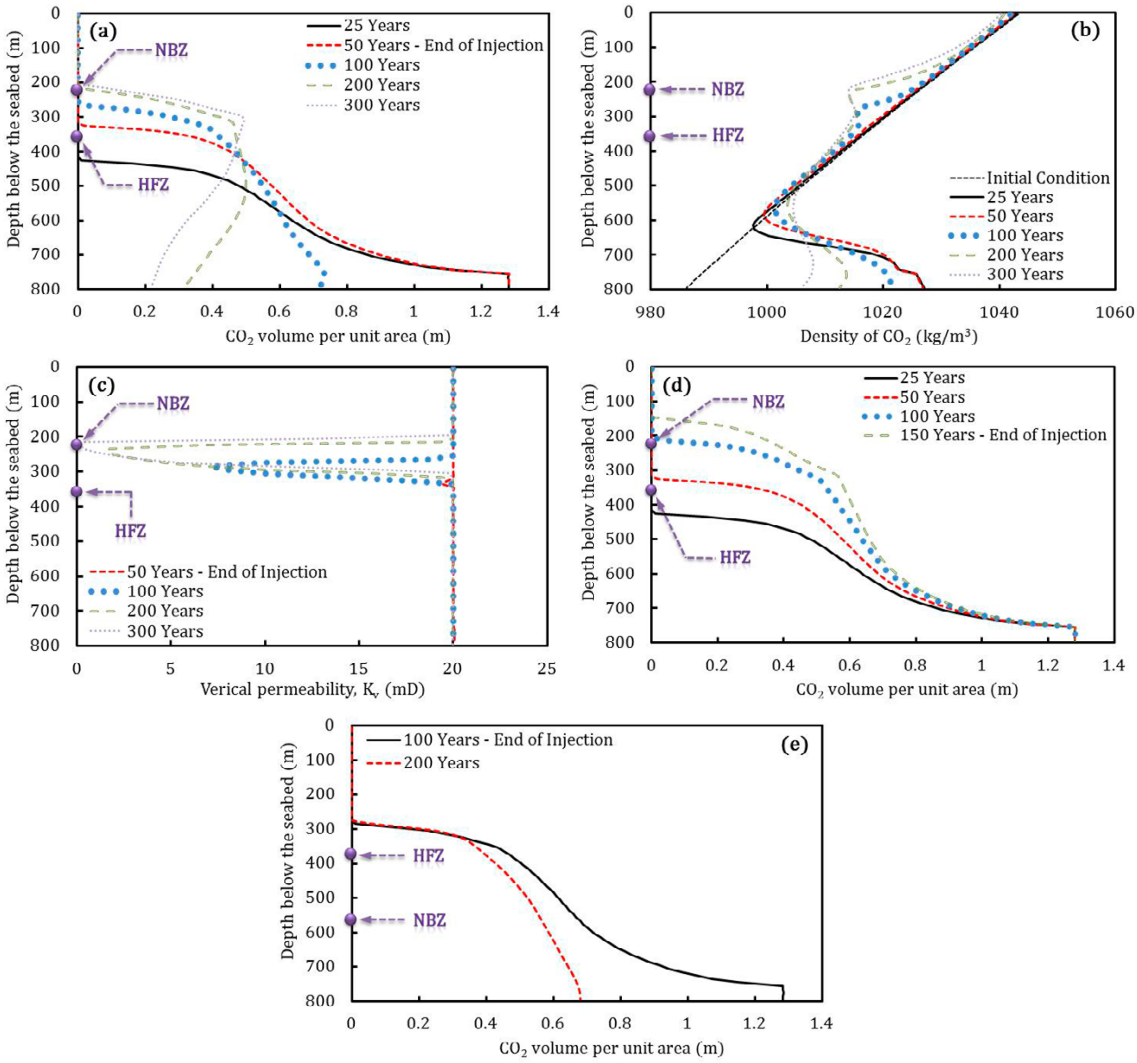

Figure 3 Simulation results for the grids that include the well: a. distribution of CO_2 volume per unit area of the grid block for Case 1 (injection lasts up to 50 years), b. density of CO_2 at the temperature-pressure conditions of the formation at different times for Case 1, c. reduction of formation permeability with hydrate formation for Case 1, d. distribution of CO_2 volume per unit area of the grid block (injection continues for 150 years), e. distribution of CO_2 volume per unit bulk area of the grid block (Case 2)

could reduce vertical flow. For Case 1 where the HFZ > NBZ, it is expected that as the CO_2 moves upward, it first reaches at a depth where hydrate forms and permeability is reduced. In Case 2 where HFZ < NBZ, it is expected that the CO_2 would be trapped below the NBZ, and would never reach the HFZ to form hydrate. In the following, we examine how the changes in pressure and temperature as a result of injection and hydrate formation could affect this.

Figure 3a shows the CO_2 volume distribution for the grids that include the well for Case 1 during the 50 years of injection and subsequent shut-in periods. Pressure driving force causes the CO_2 front to rise quickly while injection.

Figure 3a shows that HFZ cannot completely prevent upward flow of CO_2 for the current hydrate formation rate. The reduction of permeability observed in Figure 3c is not sufficient to trap the upwards flowing CO_2. The figure also shows that NBZ does not attain its initially calculated thickness (i.e. 225m). The reason is that the heat evolved

during hydrate formation in HFZ increases the temperature of the system and consequently decreases the density of CO_2 (Figure 3b).

If injection is continued for another 100 years, the CO_2 volume distribution shown in Figure 3d indicates that, CO_2 flows further higher into the initially calculated HFZ and NBZ.

Case 2 results are shown in Figure 3e, and indicate that injection of CO_2 leads to upwards movement of the CO_2 into the NBZ (of 565m). The pressure gradients caused by injection overcome the gravity force, and push CO_2 into where it is heavier than the surrounding water. Results in Figure 3e indicate that the heavier CO_2 flows into the NBZ until it reaches to HFZ (at 376m). There, reduction in permeability reduces potential for leakage. An interesting feature of super-deep disposal of CO_2 studied here is that CO_2 remains denser than water in HFZ even with the effects of increased temperature caused by hydrate formation. In contrast to the case of deep sub-seabed disposal, hydrate formation in the case of super-deep ocean acts perfectly and traps the CO_2 (Figure 3e). The reason is that the minimum temperature requirement for gravitational instability of CO_2 at this range of water depth is higher than the equilibrium temperature for hydrate.

The total CO_2 injected over the 50 and 100 years considered in Cases 1 and 2 are 55 and 110 MTonnes, respectively.

8. Conclusions

In this study, the idea of permanent storage of CO_2 in ocean sediments was numerically modelled and the fate of injected CO_2 was simulated. It was demonstrated that two important thermodynamic barriers (Hydrate Formation Zone and Negative Buoyancy Zone) are developed in the upper parts of deep and super-deep ocean sediments, which restrict upwards flow of CO_2 towards the seabed. However, the numerical results indicated that the hydrate formation zone and negative buoyancy zone estimations are not static quantities. Pressure and temperature changes as a result of CO_2 injection and hydrate formation could lead to CO_2 movement towards the seabed, more than predicted by these static estimates. This study demonstrated an example of use of a numerical simulator that allowed design of CO_2 injection depth and rate to avoid flow to the seabed. An opportunity for storage of large volumes of CO_2 was demonstrated.

9. Acknowledgement

The first author acknowledges the scholarship from the National Iranian Oil Company (NIOC) that provided the opportunity for the early stages of this study.

10. References

1. House KZ, Schrag DP, Harvey CF, Lackner KS. Permanent Carbon Dioxide Storage in Deep-Sea Sediments. Applied Physical Sciences 2006; 103 (33): 12291-5.
2. Schrag DP. Preparing to Capture Carbon. Science 2007; 315.
3. International Energy Agency (IEA). Key World Energy Statistics. 2007.
4. Organization of Petroleum Exporting Countries (OPEC). World Oil Outlook 2008.
5. British Petroleum (BP). BP Statistical Review of World Energy June 2008. 2008.
6. ExxonMobil. The Outlook for Energy: A View to 2030. 2007.
7. Wigley TML, Jones PD, Raper SCB. The Observed Global Warming Record: What Does it Tell Us. Proc Natl Acad Sci USA 1997; 94: 8314-20.
8. Bachu S. Screening and Ranking of Sedimentary Basins for Sequestration of CO_2 in Geological Media in Response to Climate Change. Environmental Geology 2003.
9. Anderson S, Newell R. Prospects for Carbon Capture and Storage Technologies. Annu Rev Environ Resour 2004.
10. Wright JF, Côtê MM, Dallimore SR. Overview of Regional Opportunities for Geological Sequestration of CO_2 as Gas Hydrate in Canada. 6th International Conference on Gas Hydrates (ICGH) 2008. British Colombia: Vancouver; July 2008.
11. Caldeira K. Monitoring of Ocean Storage Projects. IPCC Workshop on Carbon Dioxide Capture and Storage 2002.
12. Koide H, Shindo Y, Tazaki Y, Iijima M, Ito K, Kimura N, Omata K. Deep Sub-Seabed Disposal of CO_2 – The Most Protective Storage. Energy Convers. Mgmt 1997; 30 Suppl: S253-8.
13. Koide H, Takahashi M, Shindo Y, Tazaki Y, Iijima M, Ito K, Kimura N, Omata K. Hydrate Formation in Sediments in the Sub-Seabed Disposal of CO_2. Energy 1997; 22 (2/3): pp. 279-83.

14. Goldberg DS, Takahashi T, Slagle AL. Carbon Dioxide Sequestration in Deep-Sea Basalt. The Natl Acad Sci USA PNAS 2008; 105 No. 29.
15. Li Q, Wu Z, Li X. Prediction of CO2 Leakage During Sequestration into Marine Sedimentary Strata. Energy Conversion and Management 2009; 50, 503-9.
16. Rochelle CA, Camps AP, Long D, Milodowski A, Bateman K, Gunn D, et al. Can CO_2 Hydrate Assist in the Underground Storage of Carbon Dioxide? The Geological Society of London 2009; 319: 171-83.
17. National Institute of Standards and Technology (NIST). http://webbook.nist.gov/chemistry/. NIST Chemistry Webbook. NIST Standard Reference Database Number 69. The US Secretary on behalf of the United States of America 2008.
18. Span R, Wagner W. A new equation of state for carbon dioxide covering the fluid region from the triple-point temperature to 1100 K at pressures up to 800 Mpa J Phys Chem Ref Data 1996; 25 (6); 1509–96.
19. UCAR, Windows to the Universe. http://www.windows.ucar.edu/. Regents of the University of Michigan 2008.
20. Englezos P. Clathrate Hydrates. American Chemical Society. Ind Eng Chem Res 1993; 32 (7).
21. Sloan ED. Gas Hydrates: Review of Physical/Chemical Properties. American Chemical Society. Energy & Fuels 1998; 12: 191-6.
22. Computer Modeling Group Ltd (CMG). STARS User's Guide; Advanced Process and Thermal Reservoir Simulator. Computer Modeling Group 2008.
23. Konno Y, Masuda Y, Takenaka T, Oyama H, Ouchi H, Kurihara M. Numerical Study on Permeability Hysteresis During Hydrate Dissociation in Hot Water Injection. Proceedings of the 6th International Conference on Gas Hydrates (ICGH) 2008; British Columbia: Vancouver.
24. Konno Y, Masuda Y, Takenaka T, Oyama H, Ouchi H, Kurihara M. Relative Permeability Curves During Hydrate Dissociation in Depressurization. Proceedings of the 6th International Conference on Gas Hydrates (ICGH) 2008; British Columbia: Vancouver.
25. Davis EE, Chapman DS, Villinger H, Robinson S, Grigel J, Rosenberger A, et al. Seafloor Heat Flow on the Eastern Flank of the Juan de Fuca Ridge: Data from "Flanflux" Studies Through 1995. Proceedings on the Ocean Drilling Program. Initial Reports 1997; 168: 23-33.
26. Fisher AT. Permeability within Basaltic Oceanic Crust. American Geophysical Union. Reviews of Geophysics 1998; 36 (2): 97RG02916.
27. Aya I, Yamane K, Nariai H. Solubility of CO_2 and Density of CO_2 Hydrate at 30Mpa. Energy 1997; 22: 263-71.
28. Teng H, Yamasaki A, Chun MK, Lee H. Solubility of Liquid CO_2 in Water at Temperatures from 278 K to 293 K and Pressures from 6.44 MPa to 29.49 MPa and Densities of the Corresponding Aqueous Solutions. Academic Press Limited. J Chem Thermodynamics 1997; 29: 1301-10.
29. Diamond LW, Akinfiev NN. Solubility of CO_2 in Water from -1.5 to 100℃ and from 0.1 to 100 MPa: Evaluation of Literature Data and Thermodynamic Modeling. Fluid Phase Equilibria 2003; 208: 256-90.
30. Ohsumi T, Nakashiki N, Shitashima K, Hirama K. Density Change of Water Due to Dissolution of Carbon Dioxide and Near-Filed Behavior of CO_2 from a Source on Deep-Sea Floor. Pergamon Press Ltd. Energy Convers. Mgmt 1992; 33 (5-8): 685-90.
31. Song Y, Chen B, Nishio M, Akai M. The Study on Density Change of Carbon Dioxide Seawater Solution at High Pressure and Low Temperature. Energy 2005; 30: 2298-307.
32. Takahashi T, Goldberg D, Mutter JC. Secure, Long-Term Sequestration of CO_2 in Deep Saline Aquifers Associated with Oceanic and Continental Basaltic Rocks. SRI International Symposium Deep Sea & CO_2 2000; Mitaka. Japan.
33. Matter JM, Takahashi T, Goldberg D. Experimental Evolution of in Situ CO_2-Water-Rock Reactions During CO_2 injection in Basaltic Rocks: Implications for Geological CO_2 Storage. American Geophysical Union, Geochemistry Geophysics Geosystems 2007; 8 (2).
34. Bozzo A, Chen HS, Kass JR, Barduhn AJ. The Properties of the Hydrates of Chloride and Carbon Dioxide. Desalination 1975; 16: 303-20.
35. Wicander R., Monroe JS. Essentials of Geology. West Publishing Company. 1995.
36. Waples WD, Waples JS. A Review of Specific Heat Capacities of Rocks, Minerals, and Subsurface Fluids. Part 1: Minerals and Nonporous Rocks. International Association for Mathematical Geology. Natural Resources Research 2004; 13 (2).
37. Clauser C, Huenges E. Thermal Conductivity of Rocks and Minerals. American Geophysical Union 1995.